MULTIDISCIPLINARY SCIENCE JOURNAL

RESEARCH ARTICLE
Published Online: February 20, 2025
https://doi.org/10.31893/multiscience.2025404

The emerging role of dynamic contrast enhanced mri in differentiation between various histologic subtypes of oral cavity squamous cell carcinoma

Jubin John[a] | **Vadlamudi Nagendra**[a] ✉

[a]Department of Radio-diagnosis, Jawaharlal Nehru Medical College, DMIHER, Wardha, Maharashtra, -442001, India.

Abstract Differentiating histologic subtypes and assessing tumor grade of oral squamous cell carcinoma using conventional contrast-enhanced MRI can be challenging. Newer advanced imaging MRI technique such as dynamic contrast-enhanced MRI (DCE-MRI) provides assessment of prognosis and malignant potential of tumor by studying tissue microcirculation and blood perfusion. This study aims to determine whether dynamic contrast-enhanced (DCE) perfusion MRI can distinguish between histologic subtypes of oral cavity squamous cell carcinoma (SCC). Sixty-two patients with newly diagnosed tumor lesions underwent both conventional contrast-enhanced MRI and DCE perfusion. The DCE parameters from the tumor lesions were compared with normal tissue. A Student's t-test was used to assess statistical significance, with p-values < 0.05 considered significant. The malignancy group was further divided into low-grade and high-grade subtypes for comparison. High-grade cancers (stage I/II) significantly increased quantitative perfusion parameters (Ktrans, Ve, and Kep) compared to low-grade (Stage III/IV) subtypes which is statistically significant (p <0.001). There was no significant difference in the quantitative parameters between well-differentiated and moderately differentiated subtypes. High-grade tumors predominantly exhibited a Type III signal intensity curve. DCE MRI perfusion parameters and signal intensity curves can effectively differentiate low-grade from high-grade oral cavity SCC thereby addressing the specific diagnostic gap in field of oral malignancy.

Keywords: Ktrans, oral SCC, DCE-MRI, Kep, Ve

1. Introduction

Oral cancer ranks as the eighth most common cancer in developing nations and twelfth globally in overall cancer incidence (Ai et al., 2013; Carmeliet & Jain, 2000). Common sub-sites of oral cavity carcinoma include the lip, tongue, buccal mucosa, hard palate, floor of the mouth, alveolus, and gingiva (Chen et al., 2021). Squamous cell carcinoma (SCC) is the predominant histologic subtype of oral cavity neoplasms (Chikui et al., 2015). Premalignant lesions such as leukoplakia, erythroplakia, oral lichen planus, and oral submucous fibrosis carry varying risks of progressing to malignancy (Chikui et al., 2015; Dong Ji et al., 2019).

SCC accounts for over 90% of oral cavity cancers. The remaining oral cancers consist of salivary gland tumors, including mucoepidermoid carcinoma, adenoid cystic carcinoma, polymorphous low-grade adenocarcinoma, adenocarcinoma not otherwise specified, as well as lymphomas, metastases, melanomas, and sarcomas (Duan et al., 2017). Early diagnosis of oral cancers can significantly reduce both mortality and the morbidity associated with these diseases (Guo et al., 2020).

Even though conventional imaging provides the anatomic details, it won't be able to provide functional detailing as in the grade of tumour which will provide the disease prognosis.

Multiparametric MRI, which incorporates various anatomic and functional parameters, plays a crucial role in detecting and characterizing oral cavity lesions, as well as differentiating benign from malignant subtypes. The sensitivity and specificity of conventional MRI can be improved by integrating advanced techniques such as dynamic contrast-enhanced MRI (DCE-MRI), which provides insights into tissue cellularity, microstructure, vascularity, metabolite concentration, and tumor behavior (Guo et al., 2020).

Angiogenesis, essential for tumor survival and growth, is a key indicator of malignancy. Features of tumor microvasculature that contribute to increased permeability include a compromised or absent basement membrane, larger inter-endothelial junctions, and a lack of muscularis propria (Hagiwara et al., 2012). Studies have shown that tumor angiogenesis and biological characteristics are closely linked. Poorly differentiated tumors typically have disorganized, leaky blood vessels, while well-differentiated tumors may possess nearly normal microvasculature. The inadequate oxygen supply caused by leaky vessels contributes to tumor hypoxia. Several factors, including the fractional volume of extracellular

 Received: October 1, 2024 | Accepted: December 18, 2024

extravascular space, microvascular attenuation, vascular permeability, and blood flow, influence gadolinium leakage from intravascular to extravascular compartments (EES). DCE-MRI can assess these biological features (Knopp et al., 1999; Silverman et al., 1984).

DCE-MRI is an imaging technique that evaluates tissue microcirculation and blood perfusion. Commonly used semi-quantitative metrics include time-to-intensity curve, maximum slope, and peak time, while quantitative parameters include the volume transfer coefficient (Ktrans), rate constant (Kep), and extravascular extracellular volume fraction (Ve) (Liu et al., 2021; Maraghelli et al., 2022). Malignant tumors are often characterized by high vascularity, cellularity, and increased micro-vessel density. DCE-MRI can indicate malignancy through a rapid contrast wash-in (evidenced by slope and Tpeak) along with a significant peak contrast enhancement (CImax) and sustained plateau (Misra et al., 2008). Reduced differentiation in head and neck SCC is associated with increased permeability (Montero & Patel, 2015).

Following intravenous injection, gadolinium contrast agent (GCA) passively diffuses into the EES, enhancing tissue signal intensity by altering the relaxation rates of water protons. The distribution of GCA within tissues affects relaxation and signal intensity. The transfer constant from plasma to EES (Ktrans) reflects this process. As intravascular GCA concentration decreases, GCA returns from the EES to the plasma (Naumova et al., 2013).

This study aims to evaluate the utility of qualitative and quantitative DCE-MRI parameters in differentiating the histologic grading of oral cavity SCC.

2. Materials and Methods

2.1. Patient selection

This prospective study was conducted in the Department of Radiodiagnosis at a tertiary care hospital, following approval from the ethics committee. Patients with clinically suspected oral cavity neoplasia underwent multiparametric MRI examinations. MRI scans, utilizing both standard and advanced MR sequences, were performed on 65 patients. Of these, two patients did not have histopathological confirmation, and one patient had chronic kidney disease, which contraindicated the use of MRI contrast. As a result, 62 patients who met the inclusion and exclusion criteria, with available histopathological reports, were included in the analysis for MRI characteristics. The objective of the study was to characterize oral cavity lesions using conventional and advanced MRI parameters.

2.1.1. Inclusion criteria

- Patients with a radiological diagnosis of oral cavity tumors.
- Incidentally diagnosed oral cavity tumors on CT.
- Age >= 18 years.

2.1.2. Exclusion criteria

i. Any tumors arising outside the anatomical limit of the oral cavity.
ii. Age <18 years.
iii. Contraindications to MRI - cardiac pacemaker, automatic implantable cardiac defibrillator, artificial heart valve, dental or joint prosthesis (relative contraindication), cochlear implants, hearing aids, neurostimulators, insulin pump bio stimulator, intracranial aneurysm clips, claustrophobia, pregnancy, chronic renal disease.
iv. Patients who are non-cooperative for MRI.

2.1.3. Examination protocol

A 3T Magnetic Resonance Imaging scanner (Discovery MR750w GEM - 70 cm - 3.0 T MRI scanner, GE, Chicago, Illinois, United States) was used for this study. The MRI protocol included axial T1, axial T2, axial DWI, axial SWI, coronal T2, sagittal T1, sagittal T2, axial STIR, and axial DCE sequences. After administering gadopentetate dimeglumine contrast, additional axial T1 post-contrast (PC), coronal T1 PC, and sagittal T1 PC sequences were obtained. The DCE MRI was performed with the following parameters: a field of view (FOV) of 200 x 200 mm, 1 excitation, TR/TE of 167/8.5 milliseconds, a flip angle of 150°, slice thickness/gap of 5/0.5 mm, and 3 slices. Twenty scans were acquired at intervals of 8–10 seconds for each patient. A gadolinium-based contrast medium at a dose of 0.1 mmol/kg was injected intravenously at a rate of 2 mL/s using an automated injector, followed by a 20 cc saline flush.

2.1.4. Post data processing

The DCE MRI data were post-processed using the GenIQ software. The region of interest (ROI) was precisely located within the enhancing solid part of the tumor. To ensure accurate ROI placement, boundaries between the enhancing tumor and surrounding normal tissue were defined using enhanced T1-weighted and axial STIR images. Three ROIs were placed at different locations within the enhancing tumor, and the average of these values was calculated. Care was taken to exclude

vascular structures, necrotic areas, cystic components, and hemorrhagic regions. The tumor values were then compared to those of the corresponding contralateral normal tissue.

3. Results

3.1. Imaging findings

Among the glossal tumors, the majority (96%, n=44/46) had their epicenter located in the anterior two-thirds of the tongue, while the remaining (4%, n=2/46) were situated in the posterior or base of the tongue. Of the glossal tumors, 37% (n=17/46) crossed the midline lingual septum to involve the opposite hemitongue, whereas 63% (n=29/46) remained confined to the same hemitongue. The tumor extension patterns differed between primary glossal tumors and buccal mucosa malignancies. In the glossal tumor group, the most common site of extension was the root of the tongue (86%, n=40/46). Other less common extensions included the floor of the mouth (21%, n=10/46), the base of the tongue (39%, n=18/46), and the retromolar trigone (RMT) (13%, n=6/46). On T1-weighted imaging, the majority of tumors appeared isointense (66%, n=41/62), while 30% (n=19/62) were hypointense, and 3.2% (n=2/62) exhibited an iso-hypointense signal. On T2-weighted imaging, 96% (n=60/62) of tumors were heterogeneously hyperintense, with the remaining 4% (n=2/62) showing a hyperintense appearance.

3.2. Dynamic Enhancement - DCE CURVE

The dynamic contrast enhancement (DCE) patterns of the lesions were analyzed, and signal intensity curves were plotted. These curve patterns were categorized as follows: Type I – progressive enhancement, Type II – rapid uptake followed by a plateau, and Type III – rapid uptake followed by washout. The majority of lesions displayed a Type III signal intensity curve.

In the benign lesions, the enhancement pattern followed a Type I curve. Among the dysplasia cases, 33% (n=1/3) exhibited a Type I curve, while 66% (n=2/3) showed a Type II curve. For well-differentiated squamous cell carcinoma (WDSCC), 5% (n=1/18) displayed a Type I curve, 38% (n=7/18) showed a Type II curve, and 56% (n=10/18) exhibited a Type III curve. In moderately differentiated squamous cell carcinoma (MDSCC), 47% (n=17/36) had a Type II curve, while 53% (n=19/36) displayed a Type III curve. All cases of poorly differentiated squamous cell carcinoma (PDSCC) (n=4/4) demonstrated a Type III curve (Figure 1).

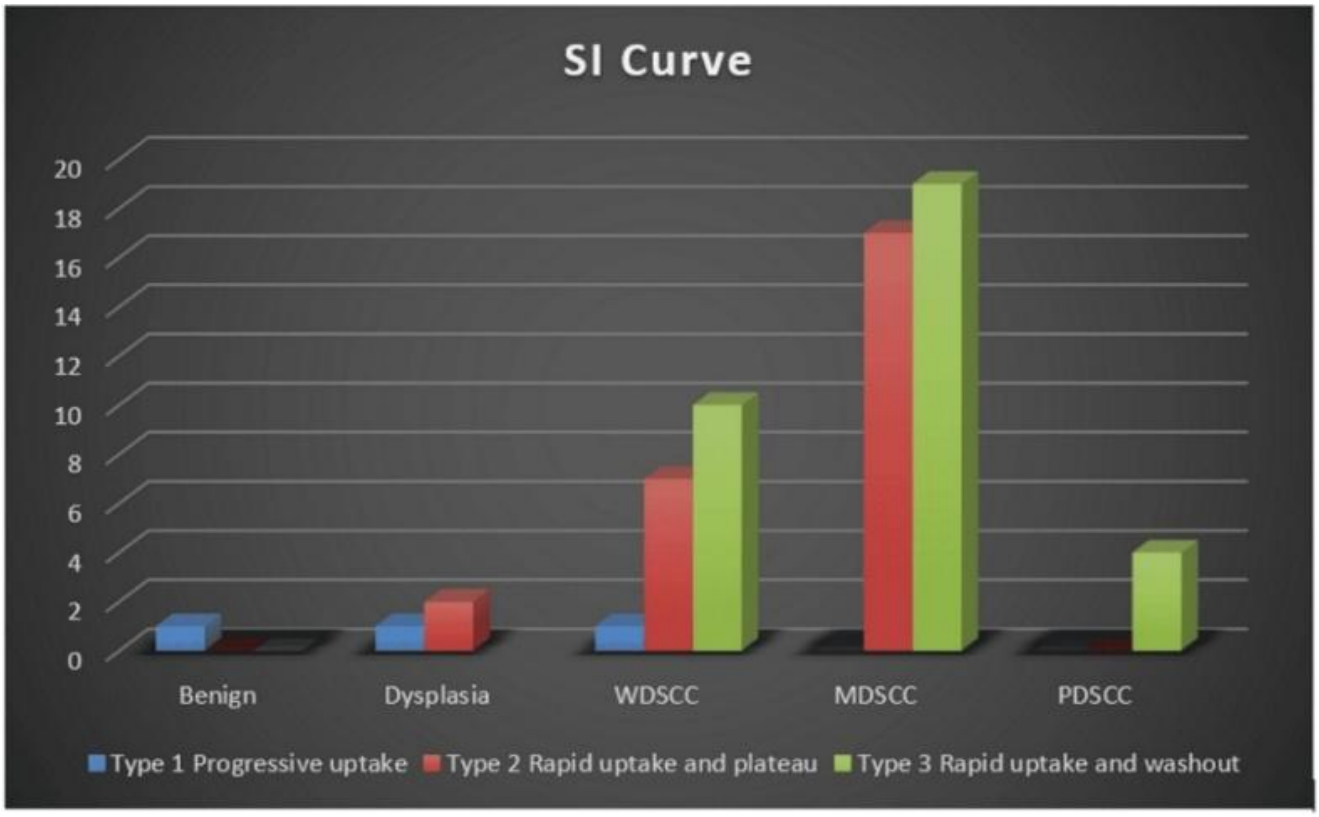

Figure 1 Bar diagram depicting the type of signal intensity graph of various histologic subtypes.

Perfusion parameters: The distribution of perfusion parameters (k trans, Ve and K ep) is depicted in (Figure 2) and (Table 1). Bar diagram depicting perfusion parameters (ktrans,Ve,Kep) comparing early stage (Stage I and II) and late stage (Stage III and IV) disease, showing significant difference of values between stages (Figure 3). An example of MRI analysis of tumor (Figure 4) with HPE correlation and DEC curve.

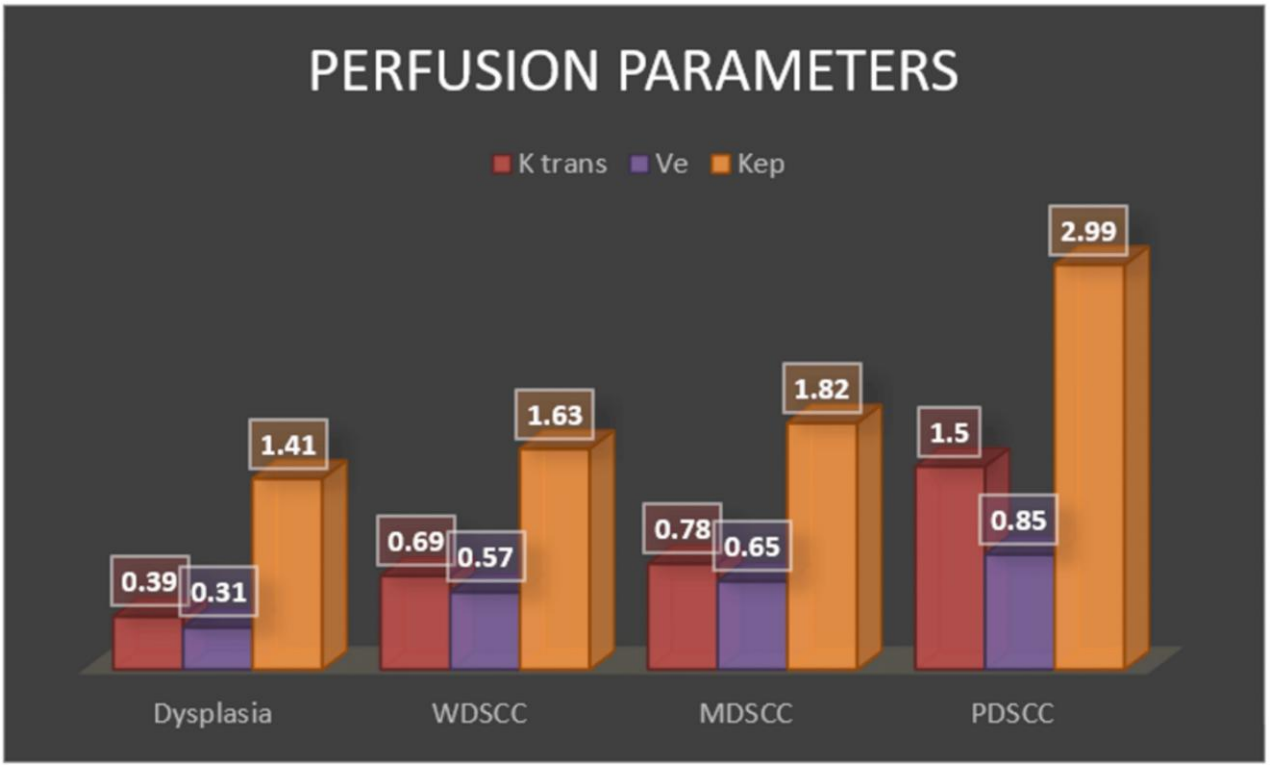

Figure 2 Distribution of perfusion parameters (k trans, Ve and K ep) in various histologic sub types.

Table 1 Perfusion parameters the distribution of perfusion parameters (k trans, Ve and K ep) is depicted in the table.

Parameters	Stage I-II (n=21)	Stage III-IV(n=40)	P value
K trans	0.54 ±0.03	1.14±0.08	<0.001
Ve	0.44±0.89	0.75±0.33	<0.001
Kep	1.52±1.01	2.35±1.03	<0.001

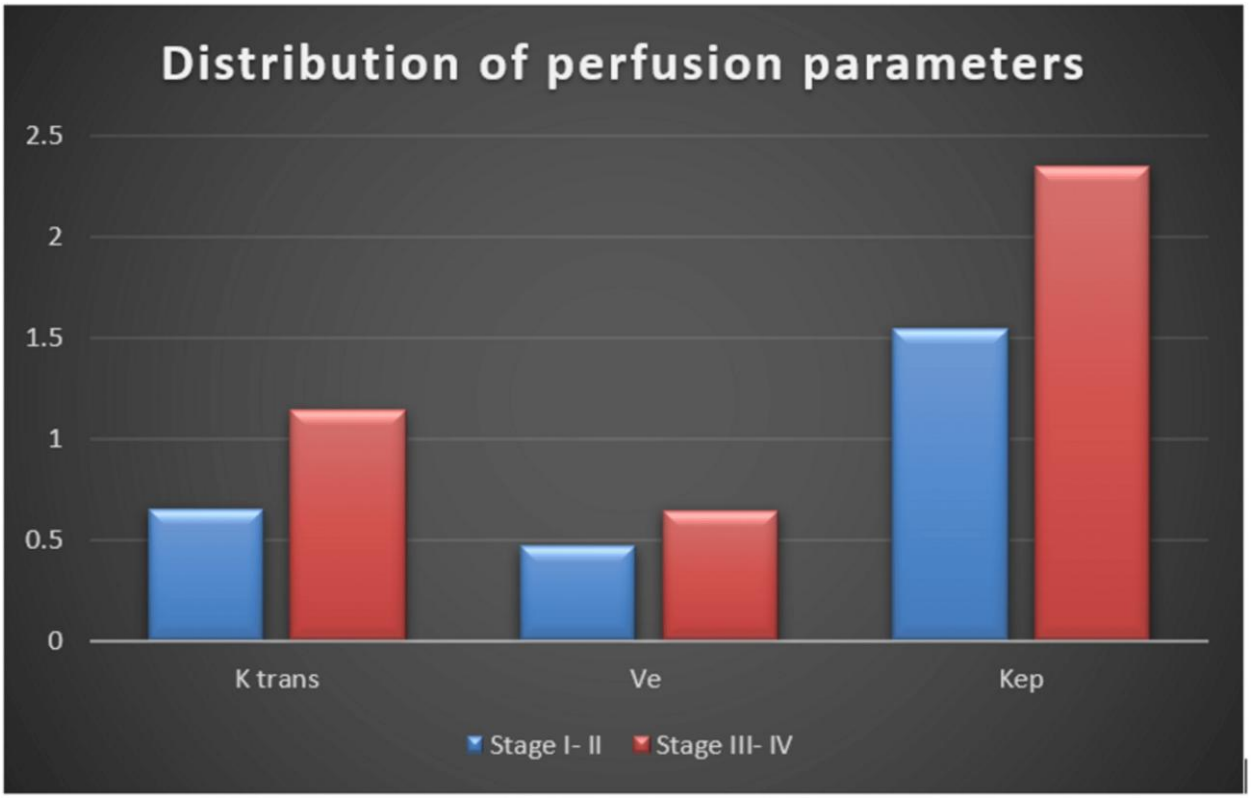

Figure 3 Showing the distribution of all perfusion parameters based on early and advanced stage tumors.

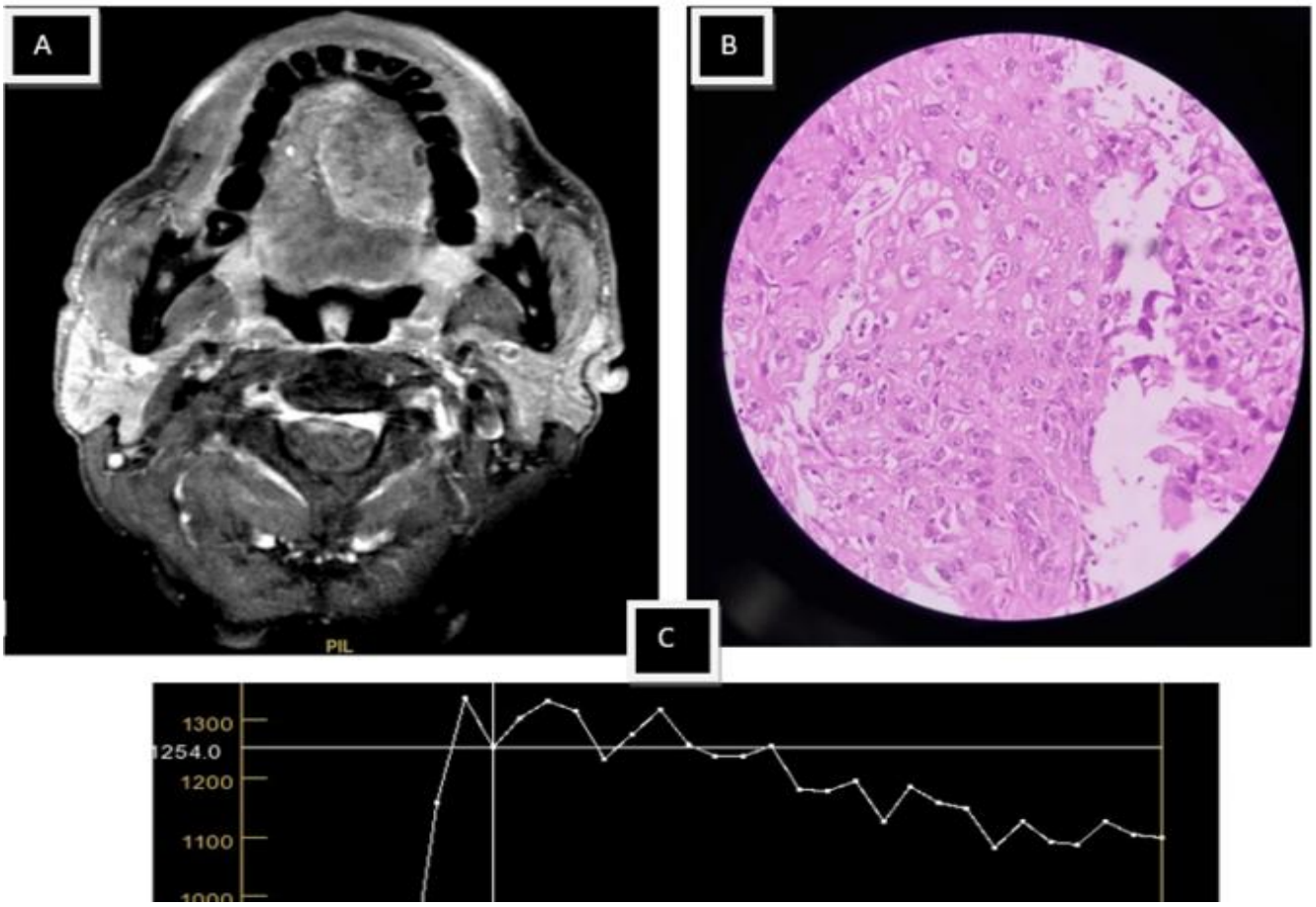

Figure 4 A. Post contrast Axial T1 FS sequence shows a heterogeneous pattern of contrast uptake. B. HPE photomicrograph shows Poorly differentiated tumor. Bits of tumor cells are arranged in sheets and scattered singly. Individual cells are large with high N:C ratio with vesicular chromatin, prominent 1-2 nucleoli and vacuolated cytoplasm. A few bizarre cells are also seen. C. DCE curve shows Type III curve with rapid contrast uptake with washout.

4. Discussion

Dynamic contrast-enhanced MRI (DCE-MRI) enables the non-invasive evaluation of tumor permeability and blood flow, providing valuable functional information about lesion characteristics. Tumors often exhibit abnormal microvasculature features, such as a disrupted or absent basement membrane, enlarged inter-endothelial junctions, and a lack of muscularis propria, all of which contribute to increased permeability (Hagiwara et al., 2012). The biology of a tumor and the degree of angiogenesis are closely linked. Well-differentiated tumors tend to maintain relatively normal microvasculature, whereas poorly differentiated tumors present with disorganized and leaky vessels. These leaky vessels can worsen tumor hypoxia due to their reduced ability to deliver oxygen effectively. Gadolinium leakage from the blood vessels into the extravascular extracellular space (EES) is influenced by factors such as fractional EES volume, microvascular density, vascular permeability, and tissue blood flow. DCE-MRI is used to assess these biological characteristics, offering insights into the vascular properties of tumors (Knopp et al., 1999; Silverman et al., 1984).

Quantitative parameters that are frequently utilized are extravascular extracellular volume fraction (Ve), rate constant (Kep), and volume transfer constant (Ktrans) (Liu et al., 2021; Maraghelli et al., 2022). (Table 2) showing differences in perfusion parameters of various stages in multiple studies with their correlation.

In the study done by Xiao Dong Ji (16), the quantitative perfusion parameters correlated well with the histological grade of tumors. The value of K trans was (0.383 ±0.074 min-1) in poorly differentiated tumors compared to (0.218 ±0.048 min-1) in well-differentiated tumors. This difference was statistically significant. Ve was substantially higher in poorly differentiated subtypes (0.712 ±0.150) compared to well-differentiated tumors (0.605 ±0.108). The cut-off value for k trans was 0.270 and for Ve was 0.732. Most of the malignant tumors showed type III graph especially for the poorly differentiated tumors (Dong Ji et al., 2019).

In our study, majority of the signal intensity curve which was obtained was type III. The benign lesion showed type I pattern of enhancement. In the category of dysplasia, 33% showed type I curve and 66% showed type II curve. In the group of WDSCC, 5% showed type I curve, 38% showed type II curve and 56 % type III curve. In the group of MDSCC, 47% showed type

II curve and 53 % with type III curve. All the PDSCC, showed type III curve. Similar results were obtained in our study with where there is presence of type III curve as the grade of tumor increases.

Table 2 Comparison of perfusion parameters in various tumor stages.

Author	DCE parameters	Stage I-II	Stage III-IV
(Chen et al., 2021)	K trans	1.03±0.13	1.70±0.16
	K trans	1.099 ±0.359	0.821±0.278
(Liu et al., 2021)	Ve	0.682±0.211	0.617±0.171
	Kep	1.688±0.406	1.443±0.483
	K trans	0.149 ±0.080	0.106±0.057
	Ve	0.219±0.140	0.188±0.148
(Guo et al., 2020)	Kep	0.806±0.247	0.641±0.221
(Maraghelli et al., 2022)	K trans	0.149 ± 0.080	0.106 ± 0.057
	K trans	0.651±0.23	1.21±0.46
	Ve	0.465± 0.13	0.64± 0.18
Our study	Kep	1.545±0.54	2.35±0.89

K trans threshold of 0.484 was used to differentiate between glossitis and tongue malignancy by Lui Fenghai et al (19). In our study mean k trans was 0.81 which was well above this threshold of 0.484, which was taken for differentiation of benign from malignant glossal tumors (Liu et al., 2021).

Our study dataset did not have any lesion of benign category. Hence, we could not arrive on a cutoff value to differentiate between benign and malignant category. However, the previously reported 19 cut-off of k-trans for labeling a lesion as malignant was valid when compared to the k trans values of our study.

The cut-off values in our study were calculated for normal vs abnormal (malignant) areas since we did not have benign oral tumors. Therefore, our calculated cut off values was lower as compared with the study of (Dong Ji et al., 2019). Our study showed a significant statistical difference ($p< 0.05$) between the normal and malignant area. Similar results of statistically significant difference (<0.001) were reported by (Chen et al., 2021) between normal area and malignant primary tumor area.

The DCE quantitative parameters in our study did not show any significant difference between the WDSCC and MDSCC tumors, which was not in correlation with any of the previously published literature. However, the overall trend was in positive correlation with the histologic grade, which was in line with the studies (Chen et al., 2021; Dong Ji et al., 2019) and Chih-Feng Chen et al (18). However, the results of the available studies (Chikui et al., 2015; Guo et al., 2020; Liu et al., 2021), Fenghai Liu et al (19) and T Chikui et al (24) showed a negative correlation with the histologic grade. All perfusion parameters of these two studies were high in the early stage rather than high grade as showed in Table 2, however these studies were inferior with low sample size to substantiate the outcome. After thoroughly reviewing these studies, we revisited a few of our cases and studied the outliers present in our perfusion parameters. Outliers are unavoidable variables in statistical studies, which are extreme values from the normal distribution (Warnakulasuriya et al., 2007). We found the presence of outliers in WDSCC and MDSCC tumors using the formula applied in excel software. These selected cases had histopathology reports done from a different lab. After eliminating the three outliers from the dataset, the trend of the DCE parameters with the histologic grade was revaluated. There was a shift from previous plateauing between WDSCC and MDSCC to a rising uniform trend similar to previously mentioned studies.

The DCE provided quantitative parameters for such clinical applications, but multiple more studies may be required in a uniform protocol across the centers so as to establish a specific trend for the histology to move from stage I to IV.

The mean k trans values showed subtle changes in its quantitative values in various subsites, which was found in our study also. There was significant ($p < 0.05$) difference between the perfusion parameters between normal area and the lesion. The values were noted for glossal and gingivobuccal tumors separately and are listed below (Table 3). Perfusion parameters of gingivobuccal tumours in our study compared with normal area, where lesion shows values significantly above cut off (Table 4).

Table 3 Perfusion parameters of glossal tumors in our study.

Parameter	Normal area	Lesion	Cut off
K trans	0.138 ± 0.08	0.81± 0.64	0.175
Ve	0.312±0.139	0.559±0.240	0.378
Kep	0.602±0.325	1.813±1.34	0.665

Table 4 Perfusion parameters of gingivobuccal tumors in our study.

Parameter	Normal area	Lesion	Cut off
K trans	0.302 ± 0.702	0.813± 0.41	0.378
Ve	0.315±0.171	0.603± 0.219	0.386
Kep	0.581±0.514	1.674±0.99	0.688

K trans and Ve were higher in gingivobuccal tumors as compared with the glossal tumors and Kep was higher in glossal tumors in our study. In the study of (Chikui et al., 2015), the value of k trans was higher in glossal tumors, whereas Ve was higher in gingivobuccal tumors. The possible explanation for alteration in perfusion parameters might be due to the increased capillary permeability due to dense and wide loops of vessels beneath the tongue epithelium in contrast to the buccal mucosae (Weber et al., 2003). However, variation between the perfusion parameters based on the change in subsite could not be explained. As a result, this noninvasive imaging method provides the treating or referring physician with the right channelization, which improves patient outcomes by enabling early prognostication of minor lesions and the initiation of suitable treatment.

Based on the study of Romeo et al. (2022), there is still no sufficient evidence and resources to promote the use of PWI (perfusion weighted imaging), like DCE in clinical practice. PWI can depict areas of tumor hypoxia which could reduce the response to chemotherapy and radiation therapy, both treatments requiring an adequate blood and oxygen supply to the tumor to be effective. Therefore, PWI might be helpful in the early assessment of therapy outcome.

Experts further encourage a standardized use of PWI across research and clinical centers to produce more robust evidence, preferably by way of multicenter/multiplatform studies in order to assess the clinical value of this challenging and promising functional MR technique for future applications in head and neck.

4.1. Study limitations

The limitations of this study on the role of dynamic contrast-enhanced (DCE) MRI in differentiating histologic subtypes of oral cavity squamous cell carcinoma (SCC) include the relatively small sample size, which may limit the generalizability of the findings. Additionally, the study did not account for variations in tumor biology that may affect perfusion parameters, potentially leading to variability in the interpretation of DCE metrics like Ktrans, Ve, and Kep. Furthermore, manual placement of regions of interest (ROIs) may introduce operator-dependent variability. The lack of longitudinal follow-up to assess how these DCE parameters correlate with treatment response and patient outcomes is another limitation. Finally, while DCE-MRI provides valuable functional insights, it should be interpreted alongside other imaging modalities and histopathologic data for a more comprehensive assessment.

5. Conclusions

In conventional non-contrast MRI sequences, T2-weighted imaging (T2WI) provides better delineation of lesions than T1-weighted imaging (T1WI). Dynamic contrast-enhanced (DCE) MRI, along with its perfusion metrics—such as Ktrans, Ve, and Kep—can effectively demonstrate tumor angiogenesis and vascular function. High-grade tumors are typically associated with a Type III signal intensity curve and elevated perfusion parameters, suggesting the potential for non-invasive tumor grade prediction. This information is crucial for treatment planning and can ultimately improve clinical outcomes. Incorporating functional MRI techniques like DCE-MRI into the traditional MRI approach significantly enhances diagnostic accuracy. However, all MRI parameters, including DCE, should be used in conjunction with conventional MRI sequences rather than in isolation for optimal diagnostic results.

Acknowledgment

I would like to thank my Department of Radio-diagnosis and my mentor Dr RPD for guiding me throughout our research.

Ethical considerations

The Institute Ethics Committee approval was obtained from All India Institute of Medical Sciences, Raipur, reference number AIIMSRPR/IEC/2020/647.

Conflict of Interest

The authors declare no conflicts of interest.

Funding

This research did not receive any financial support.

References

Ai S, Zhu W, Liu Y, Wang P, Yu Q, Dai K. Combined DCE- and DW-MRI in diagnosis of benign and malignant tumors of the tongue. *Front Biosci (Landmark Ed)*. 3;18:1098-111.

Carmeliet P, Jain RK. Angiogenesis in cancer and other diseases. *Nature*. 2000;249-57. doi:10.1038/35025220

Chen CF, Peng SL, Lee CC, Lui CC, Huang HY, Chien CY. Dynamic contrast-enhanced magnetic resonance imaging in correlation with tongue cancer stages. *Acta Radiol.* 2017. doi:10.1177/02841851209751

Chen L, Ye Y, Chen H, Chen S, Jiang J, Dan G, Huang B. Dynamic contrast-enhanced Magnetic Resonance imaging for differentiating between primary tumor,

metastatic node, and normal tissue in head and neck cancer. *Curr Med Imaging Rev.* 2017;14:416-21. doi:10.2174/1573405614666171205105236

Chikui T, Kitamoto E, Kami Y, et al. Dynamic contrast-enhanced MRI of oral squamous cell carcinoma: a preliminary study of the correlations between quantitative parameters and the clinical stage. *Br J Radiol.* 2015. doi:10.1259/bjr.20140814

Dong Ji X, Yan S, Xia S, Guo Y, Shen W. Quantitative parameters correlated well with differentiation of squamous cell carcinoma at head and neck: a study of dynamic contrast-enhanced MRI. *Acta Radiol.* 2018. doi:10.1177/0284185118809543

Duan C, Kallehauge JF, Bretthorst GL, Tanderup K, Ackerman JJH, Garbow JR. Are complex DCE-MRI models supported by clinical data? *Magn Reson Med.* 2017;77:1329-39. doi:10.1002/mrm.26189

Guo N, Zeng W, Deng H, et al. Quantitative dynamic contrast-enhanced MR imaging can be used to predict the pathologic stages of oral tongue squamous cell carcinoma. *BMC Med Imaging.* 2019.

Guo N, Zeng W, Deng H, et al. Quantitative dynamic contrast-enhanced MR imaging can be used to predict the pathologic stages of lingual squamous cell carcinoma. *BMC Med Imaging.* 2020.

Hagiwara M, Nusbaum A, Schmidt BL. MR assessment of oral cavity carcinomas. *Magn Reson Imaging Clin N Am.* 3:473-94. doi:10.1016/j.mric.2012.05.003

Jr SS, Gorsky M, Ms FL. Oral leukoplakia and malignant transformation. A follow-up study of 257 patients. *Cancer.* 1984;53:563-8. doi:10.1002/1097-0142(19840201)53:3<563::AID-CNCR2820530332>3.0.CO;2-F

Knopp MV, Weiss, et al. Pathophysiologic basis of contrast enhancement in breast tumors. *J Magn Reson Imaging.* 1999;10:260-6. doi:10.1002/(SICI)1522-2586(199909)10:3<260::AID-JMRI6>3.0.CO;2-7

Liu F, Zhao M, Lu S, Kang L. Study on the value of DCE-MRI in differentiating glossitis and tongue cancer and the intratumour heterogeneity. *Cancer Manag Res.* 2021.

Maraghelli D, Pietragalla M, Calistri L, et al. Techniques, tricks, and stratagems of oral cavity computed tomography and magnetic resonance imaging. *Appl Sci.* 2022;12. doi:10.3390/app12031473

Misra S, Chaturvedi A, Misra NC. Management of gingivobuccal complex cancer. *Ann R Coll Surg Engl.* 2008;90:546-53. doi:10.1308/003588408X3011

Montero PH, Patel SG. Cancer of the oral cavity. *Surg Oncol Clin N Am.* 2015;24:491-508.

Naumova EA, Dierkes T, Sprang J, Arnold WH. The oral mucosal surface and blood vessels. *Head Face Med.* 2013;9:1-5.

Paldino MJ, Barboriak DP. Fundamentals of quantitative dynamic contrast-enhanced MR imaging. *Magn Reson Imaging Clin N Am.* 2009;17:277-89. doi:10.1016/j.mric.2009.01.007

Parkin DM, Pisani P, Ferlay J. Estimates of the worldwide incidence of 25 major cancers in 1990. *Int J Cancer.* 1999;80:827-41. doi:10.1002/(SICI)1097-0215(19990315)80:6<827::AID-IJC6>3.0.CO;2-P

Patankar TF, Haroon HA, Mills SJ, Balériaux D, Buckley DL, Parker GJ, Jackson A. Is volume transfer coefficient (Ktrans) related to histologic grade in human gliomas? *Am Soc Neuroradiology.* 2005;2455-65.

Romeo V, Stanzione A, Ugga L, et al. Clinical indications and acquisition protocol for the use of dynamic contrast-enhanced MRI in head and neck cancer squamous cell carcinoma: recommendations from an expert panel. *Insights Imaging.* 2022;13:198. doi:10.1186/s13244-022-01317-1

Sinha AK, Jain RR, Pradhan SK. Epidemiological trend of cancer among patients at regional cancer center, Dr. B. R. Ambedkar memorial hospital, Raipur: A tertiary care hospital of central India. *Int J Heal Sci Res.* 2022;8:53-9.

Trotta BM, Pease CS, Rasamny JJ, Raghavan P, Mukherjee S. Oral cavity and oropharyngeal squamous cell cancer: key imaging findings for staging and treatment planning. *RadioGraphics.* 2011. doi:10.1148/rg.312105107

Wada K. Outliers in official statistics. *Japanese J Stat Data Sci.* 2020;669:91.

Warnakulasuriya S, Johnson NW, Van Der Waal I. Nomenclature and classification of potentially malignant disorders of the oral mucosa. *J Oral Pathol Med.* 2007;36:575-80. doi:10.1111/j.1600-0714.2007.00582.x

Weber AL, Romo L, Hashmi S. Malignant tumors of the oral cavity and oropharynx: clinical, pathologic, and radiologic evaluation. *Neuroimaging Clin N Am.* 2003;13:443-64.

Yabuuchi H, Fukuya T, Tajima T, Hachitanda Y, Tomita K, Koga M. Salivary gland tumors: diagnostic value of gadolinium-enhanced dynamic MR imaging with histopathologic correlation. *Radiology.* 2003;226:345-54. doi:10.1148/radiol.2262011486